JOURNAL OF MATERIALS SCIENCE 17 (1982) 2218–2226

Non-equilibrium crystalline superconductors in Zr–Si binary alloys rapidly quenched from melts

A. INOUE, Y. TAKAHASHI*, N. TOYOTA, T. FUKASE, T. MASUMOTO
*The Research Institute of Iron, Steel and Other Metals, and the *Graduate School, Tohoku University, Sendai 980, Japan*

The new non-equilibrium superconductor with a b c c structure has been found in rapidly quenched Zr–Si alloys. The silicon content in the b c c alloys was limited to the narrow range between 8 and 11 at%. The b c c alloys showed a superconducting transition whose temperature increased from 3.20 to 3.84 K with decreasing silicon content. The upper critical magnetic field and the critical current density for $Zr_{92}Si_8$ alloy were of the order of 3.58×10^6 Am^{-1} at 2.0 K and 3.3×10^6 Am^{-2} at 2.42 K in the absence of an applied field. The upper critical field gradient at the transition temperature and the electrical resistivity at 4.2 K were about -1.82×10^6 Am^{-1} K^{-1} and about 150 $\mu\Omega$cm. The Ginzburg–Landau parameter κ and coherence length $\xi_{GL}(0)$ were estimated to be about 65 and 6.3 nm, respectively, from these experimental values by using the Ginzburg–Landau–Abrikosov–Gorkov theory and hence it is concluded that the present b c c alloys are extremely "soft" type-II superconductors with a high degree of dirtiness.

1. Introduction

According to the study on the superconductivity of vapour-deposited amorphous metals and alloys by Collver and Hammond [1], it is expected that melt-quenched zirconium-based amorphous alloys exhibit superconducting transition temperatures, T_c, higher than those of the crystalline alloys. In fact, it has been recently demonstrated that the amorphous alloys of Zr–Si [2–4] and Zr–Si–M (M = B, C, Ge, Sn or Al) [5] systems obtained by a liquid quenching technique have T_c values ranging from 2.1 to 4.1 K which are about 4 to 7 times as high as that (0.61 K) [6] of pure hexagonal close packed (h c p) zirconium. In subsequent investigations, it was found that a non-equilibrium crystalline phase with a body centered cubic (b c c) structure appeared on the low metalloid concentration side of the amorphous phase-forming region, and the b c c phase also exhibited superconductivity better than that of the equilibrium crystalline phase, as well as high hardness combined with a rather ductile nature. This paper deals with the composition range for the formation of the non-equilibrium b c c solid solution in the Zr–Si bindary system and the superconducting properties and hardness of these alloys.

2. Experimental procedure

Mixtures of 99.6 wt% pure zirconium and 99.999 wt% pure silicon were melted under an argon atmosphere in an arc furnace. The ingots were repeatedly turned over and remelted to ensure homogeneity. The compositions of alloys reported are the nominal ones since the losses during melting were negligible.

Continuous ribbon specimens of about 1 mm width and 0.02 mm thickness were prepared from the master alloys under an argon atmosphere using a modified single-roller melt spinning apparatus adapted to a levitation furnace. The methods of characterizing the as-quenched phases by X-ray and electron metallographic techniques are described elsewhere [2]. Hardness was measured by a Vickers microhardness tester with a 100 g load.

The superconducting transition was detected by measuring the resistivity of the specimen using a conventional four-probe method with a constant current of 1 mA. The temperature was measured with an accuracy of ± 0.01 K using a calibrated germanium thermometer. The measurements of critical current density, $J_c(H)$, and upper critical magnetic field, $H_{c2}(T)$, were performed at various

0022–2461/82/082218–09$03.58/0

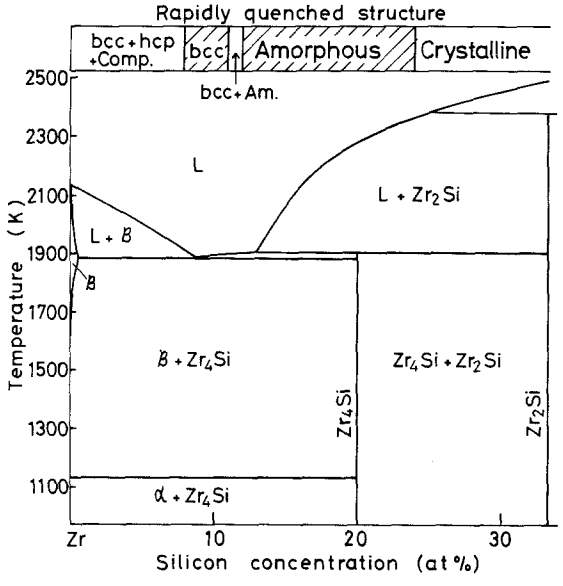

Figure 1 Composition range for the formation of a b c c single phase in the Zr–Si binary system. The binary phase diagram was adopted from [7].

temperatures ranging from 1.5 K to T_c using a superconducting solenoid for magnetic fields up to about 7.16×10^6 Am^{-1} applied transversely to the specimen.

3. Results

3.1. Structure and formation range of the non-equilibrium crystalline phase

The compositional dependence of as-quenched phase in the Zr–Si binary system is illustrated in Fig. 1: the equilibrium phase diagram [7] is also given for comparison. In the alloy system, it can be seen that the amorphous and b c c phases appear as a non-equilibrium phase instead of the equilibrium mixture of h c p α-zirconium and Zr_4Si phases. Their formation is limited to a range of 8 to 11 at% Si for the b c c phase and of 12 to 25 at% Si for the amorphous phase.

The microstructure of the b c c phase in $Zr_{91}Si_9$ alloy is shown in Fig. 2, together with the corresponding selected area diffraction pattern. In the figure, the mixed structure consisting of h c p α-zirconium, b c c β-zirconium and an unidentified Zr–Si compound in $Zr_{94}Si_6$ alloy, and the amorphous single phase of the $Zr_{85}Si_{15}$ alloy are given for reference. As shown in Fig. 2c, the b c c phase contains numerous internal defects and the diffraction pattern taken by using an aperture having a diameter of about 0.2 μm shows many reflection spots which extend along the circumferential direction, indicating that the b c c single phase consists of numerous subgrains with sizes less than about 100 nm. The lattice parameter measured by the X-ray diffractometer technique tends to increase with increasing silicon content, e.g., 0.3547 nm for $Zr_{91}Si_9$ and 0.3550 nm for $Zr_{89}Si_{11}$. The b c c lattice parameter can be extrapolated to a value of about 0.3533 nm for the hypothetical pure b c c zirconium. Although the lattice parameters of the b c c Zr–Si alloys are smaller than that (0.3609 nm) for pure b c c β-zirconium at temperatures as high as 1135 K [8], the values are much larger than the lattice parameter of hypothetical pure b c c zirconium at room temperature because of the dissolution of a large amount of silicon. The above results indicate that the b c c phase is a supersaturated solid solution containing silicon element much more than the equilibrium concentration.

3.2. Hardness

The Vickers hardness, H_v, of Zr–Si alloys showing the b c c single phase is plotted as a function of silicon content in Fig. 3: the data of the amorphous single phase [2] are also shown for comparison. The hardness of the b c c alloys increases significantly from 415 to 520 DPN with increasing silicon content. Furthermore, one can see that these values are slightly higher than those [2] of the amorphous alloys. Such high hardness values are considered to be caused by the combined effect of solid solution hardening and the extremely high density of internal defects.

It may be important to note that the non-equilibrium b c c alloys possess a relatively highly flexible nature. As an example, the deformation structure of $Zr_{89}Si_{11}$ alloy bent completely by pressing against the edge of a razor blade is shown in Fig. 4. Numerous deformation markings can be seen near the bent edge even though the occurrence of minor cracks are observed.

3.3. Electrical resistivity

The electrical resistivity, ρ, at 77 K and the temperature coefficient of resistivity (TCR) in the temperature range from 77 K to room temperature, $1/\rho_{RT}(d\rho/dT)$, for the b c c alloys are plotted as a function of silicon content in Fig. 5; the data for amorphous Zr–Si alloys are also given for comparison. The resistivity of the b c c phase is of the order of 145 to 165 μΩcm, being considerably lower than that of the amorphous phase.

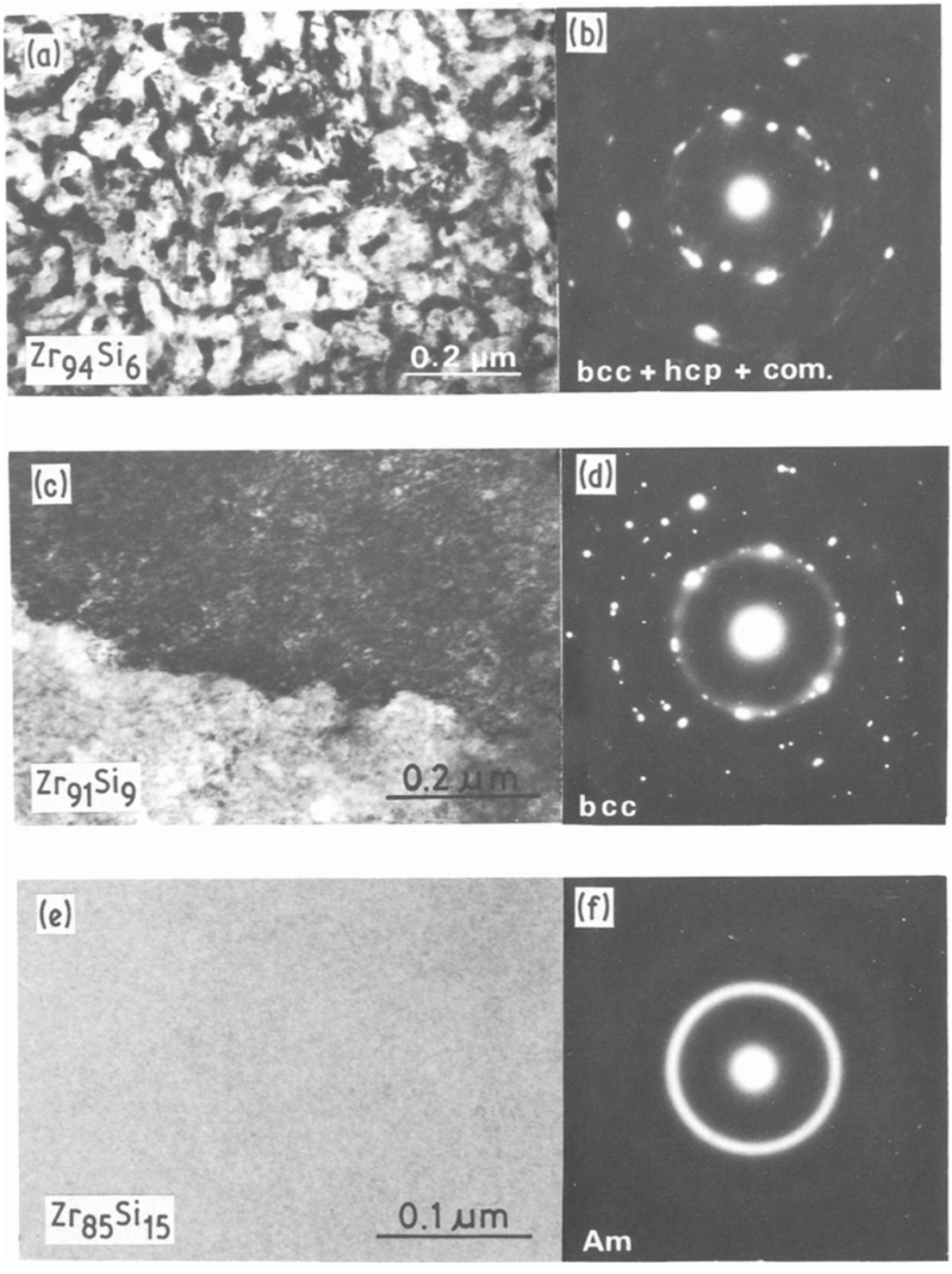

Figure 2 Transmission electron micrographs and selected area diffraction patterns showing the as-quenched structure of (a) and (b) $Zr_{94}Si_6$, (c) and (d) $Zr_{91}Si_9$ and (e) and (f) $Zr_{85}Si_{15}$ alloys.

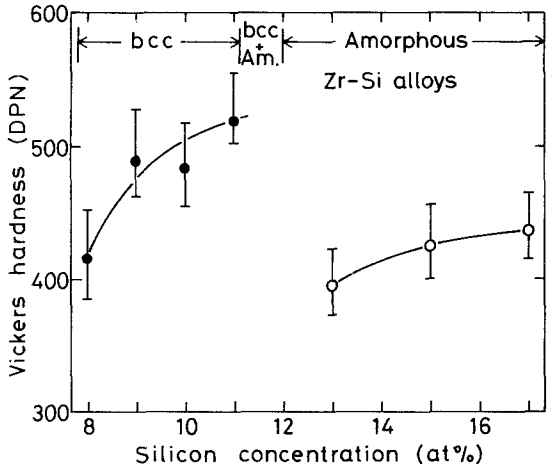

Figure 3 Change in Vickers hardness, H_v, for b c c and amorphous Zr–Si alloys with silicon content.

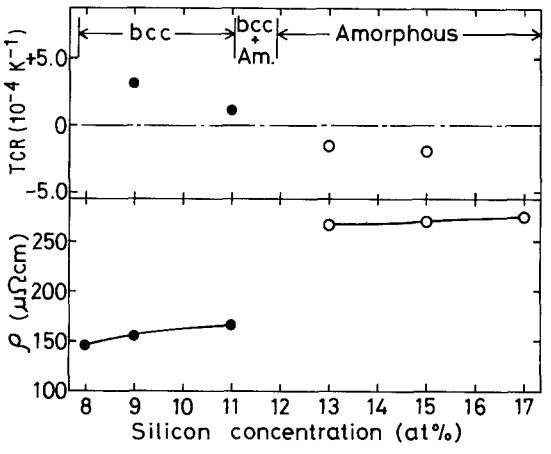

Figure 5 Changes in electrical resistivity, ρ, at 77 K and temperature coefficient of resistivity (TCR) of b c c and amorphous Zr–Si alloys with silicon content.

This suggests that the mean free path of electrons in the b c c phase is longer compared with the amorphous phase even though the former phase dissolves a large amount of silicon and contains numerous internal defects. The temperature coefficient shows positive values ranging from 1.07×10^{-4} to 3.19×10^{-4} K^{-1} and its sign is opposite to that of the amorphous alloys. It can also be seen in Fig. 5 that the TCR tends to decrease with increasing resistivity and might become zero around $\rho = 180\,\mu\Omega$cm, even though this value is slightly higher than that ($\simeq 150\,\mu\Omega$cm) for a large number of crystalline alloys [9].

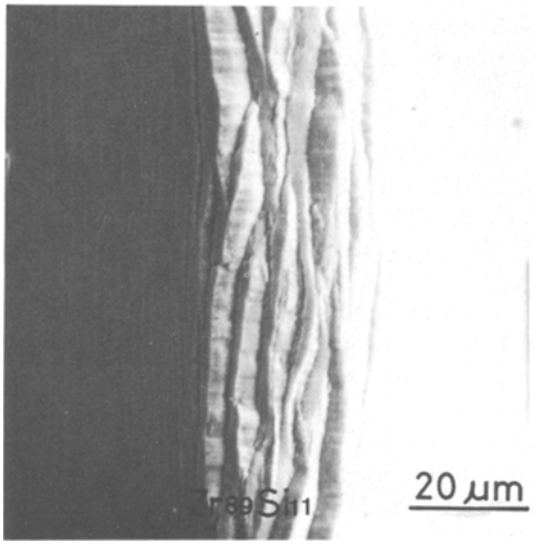

Figure 4 Scanning electron micrograph showing the deformation marking at the tip of a b c c $Zr_{89}Si_{11}$ alloy bent through 180° around the edge of a thin razor blade.

3.4. Superconducting properties

Fig. 6 shows the electrical resistance curves in the vicinity of T_c in the case of no applied magnetic field for the b c c Zr–Si alloys. The data of amorphous $Zr_{87}Si_{13}$, $Zr_{85}Si_{15}$ and $Zr_{83}Si_{17}$ alloys are also included for comparison. The transition occurs rather sharply with a temperature width of less than 0.5 K from the relatively high electrical resistivity values ($\simeq 150\,\mu\Omega$cm) of the b c c alloys. However, as seen in the figure, its width is much wider than that of the amorphous alloys. Fig. 7 shows the plots of T_c and ΔT_c of the b c c Zr–Si alloys as a function of silicon content. In addition, the data of amorphous Zr–Si alloys [2] are also plotted for reference. T_c is the temperature corresponding to $R/R_n = 0.5$, where R_n is the resistance in the normal state. The transition width ΔT_c, represented by a vertical bar in the figure, represents the temperature interval between 10% and 90% of R/R_n. T_c is 3.20 K for $Zr_{89}Si_{11}$ and increases with decreasing silicon content. The highest T_c attained is 3.84 K for $Zr_{92}Si_8$. As shown in Fig. 7, any further decrease in silicon content resulted in a significant lowering of T_c, accompanied by a structural change of the b c c single phase to the mixed structure of b c c β-zirconium, h c p α-zirconium and an unidentified Zr–Si compound. As a result, the alloy remained in a normal state down to a temperature as low as 1.5 K. Further, it may be important to note that the T_c of hypothetical pure b c c zirconium can be extrapolated to a value of 5.3 K from the variation of T_c with silicon content shown in Fig. 7. It is concluded from the above results that the non-

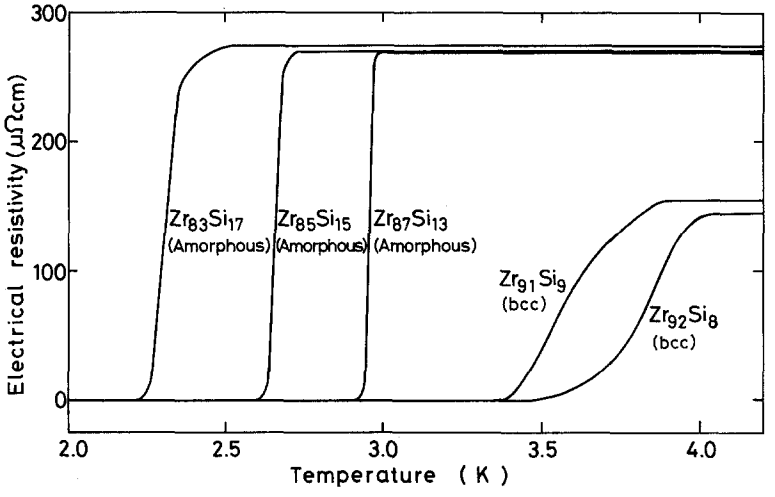

Figure 6 Electrical resistivity as a function of temperature for several Zr–Si bcc and amorphous alloys.

equilibrium bcc solid solution is a new superconductor having a T_c value much higher than that of the equilibrium phases. Furthermore, it appears important to note that the T_c values of the bcc phase lie on the linear line extrapolated based on the data of the amorphous alloys. This result suggests that the superconductivity is dominated by the same mechanism in spite of the distinct difference in as-quenched structure. The detailed discussion on this point will be presented in a later section.

The upper critical magnetic field, H_{c2}, was measured at different temperatures ranging from 1.5 K to T_c. Fig. 8 shows the transition curves from the superconducting state to the normal state through the superconducting mixed state under a current of 1 mA at different temperatures for the bcc $Zr_{92}Si_8$ alloy. Resistive states are seen in a wide range of fields and the transition is quite considerably broad. The so called "peak effect", which is one of the characteristic nature for amorphous Zr–Si superconductor [3, 4], does not appear on the resistive transition curve, indicating the existence of a rather strong flux pinning force. This tendency is considered to be due to the fact that the structure of the bcc phase is more inhomogeneous on the scale of coherence length compared with the amorphous phase. Here, we define H_{c2} to be the applied magnetic field at which the resistance of the samples begins to deviate from its normal value. The temperature dependence of H_{c2} for the bcc Zr–Si alloys is shown in Fig. 9, where the solid lines represent a linear extrapolation at T_c. H_{c2} increases linearly with decreasing temperature over almost the whole temperature range and the gradient at T_c, $(dH_{c2}/dT)_{T_c}$, is -1.75×10^6 Am^{-1} K^{-1} for $Zr_{92}Si_8$ and -1.83×10^6 Am^{-1} K^{-1} for $Zr_{91}Si_9$.

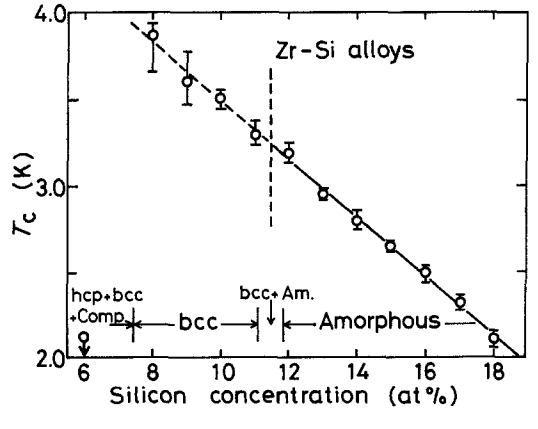

Figure 7 Changes in the superconducting transition temperature, T_c and the transition width, ΔT_c, of bcc and amorphous Zr–Si alloys with silicon content. Vertical bars represent the transition width.

The critical current density, J_c, was measured at 2.42 K and 2.87 K under an external applied magnetic field. Fig. 10 shows the critical current density, $J_c(H)$, as a function of magnetic field for the bcc $Zr_{92}Si_8$ and $Zr_{91}Si_9$ alloys. For instance, J_c at 2.42 K in the absence of an applied field is found to be about 2 to 3×10^6 Am^{-2}. The value of J_c decreases very rapidly with increasing magnetic field and at $H/H_{c2} \simeq 0.3$ it is of the order of 0.1×10^6 Am^{-2}. Such a rapid decrease of J_c with increasing field is due to the weak flux pinning force, probably because the bcc alloys have a homogeneous structure on the scale of coherence length which is estimated to be about 6.3 nm (see Section 4.1). That is, this result suggests the possibility that lattice defects in the

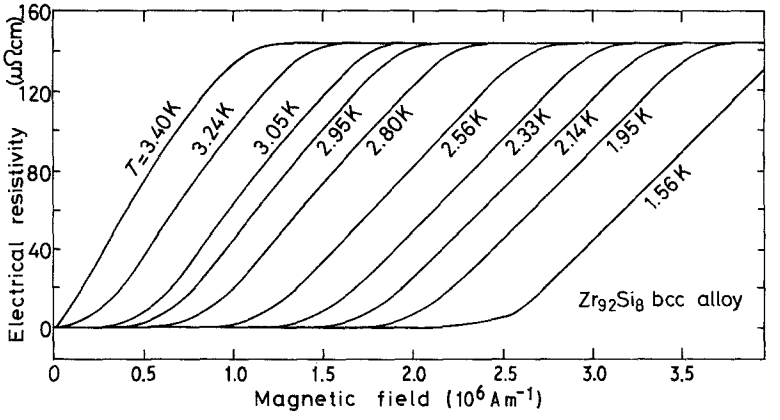

Figure 8 Resistance as a function of magnetic field for b c c $Zr_{92}Si_8$ alloy.

present b c c alloys are strongly distorted on a scale smaller than the coherence length. However, judging from the result that the J_c values of b c c alloys are higher than that of the amorphous $Zr_{85}Si_{15}$ alloy, $0.2 \times 10^6\,A\,m^{-2}$ at about 2.4 K [3, 4], it may be stated that the flux pinning force for the b c c phase is not so weak as that for the amorphous single phase because of the existence of effective pinning centres such as grain boundaries, dislocations and the other defects.

4. Discussion

4.1. Formation of the non-equilibrium b c c solid solution

As is evident from the equilibrium phase diagrams of the Zr–Si binary system, the field where the b c c phase exists stably is located at temperatures above about 1273 K and the maximum dissolution of silicon in b c c β-zirconium is limited to less than about 0.6 at% [7]. Therefore, in order to form a b c c single phase at room temperature, the equilibrium b c c phase must be cooled sufficiently rapidly to room temperature without the transformation from the b c c to the h c p phase. In addition, the formation range of the non-equilibrium b c c phase deviates significantly to the silicon rich side compared with the equilibrium phase diagram. This result indicates that the b c c phase which exists stably at high temperatures transforms to h c p α-phase and Zr–Si compound and hence no b c c single phase is produced in the equilibrium composition range of b c c phase even by the melt-

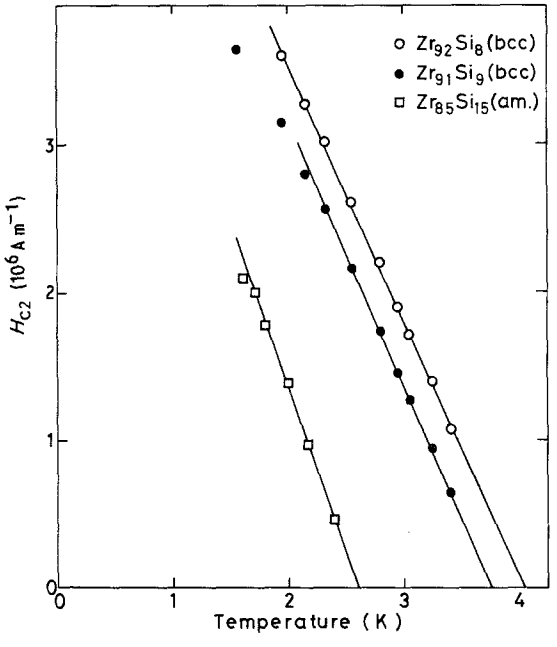

Figure 9 H_{c_2} as a function of temperature for b c c and amorphous Zr–Si alloys.

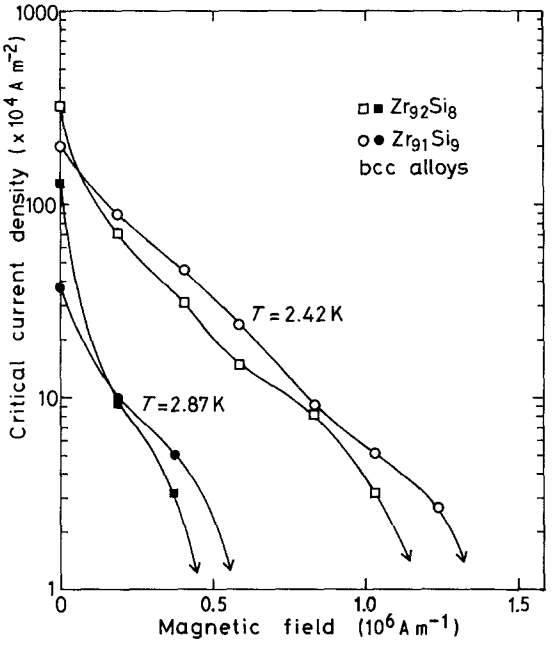

Figure 10 J_c as a function of magnetic field for b c c $Zr_{92}Si_8$ and $Zr_{91}Si_9$ alloys.

TABLE I Superconducting and the related properties of b c c and amorphous Zr–Si alloys.

Alloy system	T_c (K)	$(dH_{c2}/dT)_{T_c}$ (10^6 Am^{-1} K^{-1})	ρ, 4.2 K ($\mu\Omega$cm)	γ (J m^{-3} K^2)	$N^*(0)$ $\times 10^{41}$†	$\xi_{GL}(0)$ (nm)	κ	D (cm^2 sec^{-1})	Structure
$Zr_{92}Si_8$	3.84	−1.75	145	336.5	2.68	6.2	63	0.499	b c c
$Zr_{91}Si_9$	3.57	−1.83	155	331.0	2.64	6.3	67	0.477	b c c
$Zr_{85}Si_{15}$	2.65	−2.30	270	239.0	1.90	6.6	100	0.390	Amorphous

†$N^*(0)$: states cm^{-3} J^{-1} spin^{-1}.

quenching technique. Therefore, in order to form a b c c single phase at room temperature in the Zr–Si system, it is necessary to supercool the primary b c c phase containing silicon element more than the limits of the equilibrium solubilities, and to suppress the phase transformation of β to α + compound.

Furthermore, it can be seen in Fig. 1 that the formation range of the b c c phase is located in the vicinity of the eutectic composition and the amorphous single phase appears in the composition range which encompasses the Zr_4Si compound. This result is in disagreement with the general tendency [10] that almost all the amorphous alloys in metal–metalloid systems are located in the composition range including their eutectic point. The reason why the b c c single phase forms in place of an amorphous phase in spite of its deep trough of melting temperature near the eutectic composition appears to be due to the significantly low silicon content at the eutectic point in Zr–Si system. Considering the previous results [11] that the formation of an amorphous phase in binary alloys is commonly limited to the metalloid range about 13 to 30 at%, it may be said that the silicon content (9 at%) at the eutectic composition is too low to form the amorphous phase of Zr–Si alloys, resulting in the b c c single solid solution saturated with silicon. The importance of metalloid content and composition as well as the deep trough of melting temperature for the formation of an amorphous phase has been pointed out from the viewpoints of atomic configuration, see for example, [12] and chemical bonding nature [13] of constituent elements.

4.2. Superconducting parameters

It has been demonstrated in a previous section that the non-equilibrium b c c solid solution is a new superconductor exhibiting T_c values much higher than that of equilibrium pure zirconium metal. In this section, we shall investigate the origin of the superconductivity of the b c c solid solution by evaluating some fundamental superconducting parameters. From the measured values of the upper critical field gradient at T_c, $(dH_{c2}/dT)_{T_c}$, and electrical resistivity, ρ, we can estimate some fundamental parameters dominating superconductivity such as the electronic specific heat coefficient, γ, the electronic dressed density of states, $N^*(0)$, at the Fermi level, and Ginzburg–Landau (GL) coherence length $\xi_{GL}(0)$ and the GL parameter κ by using the following relations based on the Ginzburg–Landau–Abrikosov–Gorkov (GLAG) theory, see for example [14].

$$\gamma = -\frac{\pi^3 k_B}{12e\rho}\left(\frac{dH_{c2}}{dT}\right)_{T_c}, \quad (1)$$

$$N^*(0) = \frac{-\pi h(dH_{c2}/dT)_{T_c}}{16k_B e^2 \phi_0 \rho}, \quad (2)$$

$$\xi_{GL}(0) = \left[\frac{\phi_0}{2\pi T_c}\left(\frac{dH_{c2}}{dT}\right)^{-1}_{T_c}\right]^{1/2}, \quad (3)$$

and

$$\kappa = (6.0\gamma^{1/2})^{-1}(-dH_{c2}/dT)_{T_c}, \quad (4)$$

where h is Planck's constant, k_B is the Boltzmann constant and e is the electronic charge: the values have been obtained by the usual methods. ϕ_0 represents the flux quantum. The superconducting parameters in the b c c Zr–Si alloys obtained using these equations are summarized in Table I, and the values of T_c, $(dH_{c2}/dT)_{T_c}$, ρ and the electronic diffusivity, D, are also included for reference. The value of D is given by the following expression [15],

$$D = \frac{4k_B c}{\pi e}\left(\frac{dH_{c2}}{dT}\right)^{-1}. \quad (5)$$

κ, $\xi_{GL}(0)$ and D are about 65, 6.3 nm and 0.488 cm^2 sec^{-1} for the b c c Zr–Si alloys. Such a high value of κ and the low value of D appear to originate from a small value of the electron mean free path, l, due to the high density of lattice defects near atomic scale, as evidenced by the high electrical resistivity. Therefore, it is concluded that the new superconductor of the b c c solid solution found in the present work is of

typical type-II material characterized by a high degree of dirtiness. Furthermore, it has been demonstrated that the flux pinning force of this superconductor is very weak as is evident from the result (Fig. 8) that the resistive state generates at considerably low magnetic fields due to the flux flow. This weak flux pinning force also implies that the present crystalline superconductor is a very "soft" type-II superconductor despite the expectation that numerous internal defects introduced in the b c c phase might act as pinning centres. This unexpected result is considered to be due to the correlation between the size of these defects and the coherence length. The coherence length of the present superconductors is estimated to be about 6.3 nm and the size of these defects appears to be very small, probably less than 1 to 2 nm, from the observation that the individual defects are indistinguishable in the highly magnified electron micrographs. Hence, such a weak pinning force is considered to originate from the result that the size of lattice defects in the b c c phase is smaller than the coherence length and the b c c superconductor is homogeneous on the scale of coherence length.

Finally, the superconducting properties and the relevant properties are compared between the b c c phase and the amorphous phase in the Zr–Si alloys as represented in Table I. The γ and the $N^*(0)$ values for the b c c alloy are about 334.0 $J\,m^{-3}\,K^{-2}$ and 2.66×10^{41} states $cm^{-3}\,J^{-1}\,spin^{-1}$, being significantly higher than those of the amorphous alloy. There is a clear tendency that the larger the values of γ and/or $N^*(0)$, the higher is T_c. From this result, the reason why T_c is higher for the b c c alloy than for the amorphous alloy appears to be due to the high values of γ and/or $N^*(0)$ for the former alloy. Furthermore, while D is higher for the b c c alloy, the other parameters of $(dH_{c2}/dT)_{T_c}$, ρ, $\xi_{GL}(0)$ and κ are larger for the amorphous alloy. The reason for such differences appears to be due to the fact that the degree of distortion in the atomic configuration is much larger for the amorphous phase than for the b c c solid solution. The detailed investigation on the atomic configuration in the non-equilibrium b c c and amorphous phases will shed some light upon the further understanding of the difference in the mechanism of superconductivity.

5. Summary

Non-equilibrium b c c solid solution exhibiting superconductivity and a rather ductile nature was found in Zr–Si system. Specimens were produced in the form of a continuous ribbon of about 1 mm wide and about 0.02 mm thick by using a rapid quenching apparatus designed for high melting alloys. The formation of the b c c phase was limited to a silicon content between about 8 and 11 at%. The lattice parameter varies in the range from 0.3547 nm at 9 at% Si to 0.3550 nm at 11 at% Si. Vickers hardness was of the order of 470 DPN. The b c c alloy had rather good bend ductility and the occurrence of cracks was hardly observed even after a closely contacted bending test. In addition, the b c c solid solution showed a superconducting transition. T_c increased with decreasing silicon content and reached a maximum value of 3.84 K at 8 at% Si. From the variation of T_c with silicon content, T_c of the hypothetical pure b c c zirconium was extrapolated to be 5.3 K. The same compositional dependence was recognized for H_{c2} and J_c. The values of H_{c2} and J_c for $Zr_{92}Si_8$ were of the order of 3.58×10^6 Am^{-1} at 2.0 K and 3.3×10^6 Am^{-2} at 2.42 K in the absence of an applied field. The dH_{c2}/dT at T_c and ρ of the b c c superconductor were about -1.83 $Am^{-1}K^{-1}$ and 150 $\mu\Omega$cm. $\xi_{GL}(0)$ and κ were estimated to be about 6.3 nm and 65, respectively, from the $(dH_{c2}/dT)_{T_c}$ and ρ data by using the extend GLAG theory and it was therefore concluded that the present non-equilibrium b c c solid solutions are typical type-II superconductor with a high degree of dirtiness.

References

1. M. M. COLLVER and R. H. HAMMOND, *Phys. Rev. Lett.* **30** (1973) 92.
2. A. INOUE, Y. TAKAHASHI and T. MASUMOTO, *Sci. Rep. Res. Inst. Tohoku Univ.* **A-29** (1981) 296.
3. N. TOYOTA, T. FUKASE, A. INOUE, Y. TAKAHASHI and T. MASUMOTO, *Physica* **107B** (1981) 465.
4. A. INOUE, Y. TAKAHASHI, N. TOYOTA, T. FUKASE and T. MASUMOTO, Proceedings of the 4th International Conference on Rapidly Quenched Metals, Sendai, August 1981, edited by T. Masumoto and K. Suzuki (The Japan Institute of Metals, 1982) p. 1221.
5. A. INOUE, Y. TAKAHASHI and T. MASUMOTO, unpublished results.
6. B. W. ROBERTS, NBS Technical Note 983 (U.S. Department of Commerce, Washington) p. 12.
7. C. E. LUNDIN, D. J. MCPHERSON and M. HANSEN, *Trans. Amer. Soc. Met.* **45** (1953) 901.
8. "Metals Databook" (The Japan Institute of Metals, Maruzen, Tokyo, 1974) p. 46.

9. J. H. MOOIJ, *Phys. Stat. Sol. (a)* **17** (1973) 521.
10. C. SURYANARAYANA, "Rapidly Quenched Metals – A Bibliography 1973 – 1979" (IFI Plenum, New York, 1980).
11. H. A. DAVIES, *Phys. Chem. Glasses* **17** (1976).
12. Y. WASEDA, H. OKASAKI and T. MASUMOTO, *J. Mater. Sci.* **12** (1977) 1927.
13. H. S. CHEN, *Acta Met.* **22** (1974) 897.
14. T. R. ORLANDO, E. J. MCNIFF, Jr., S. FONER and M. R. BEASLEY, *Phys. Rev. B* **19** (1979) 4545.
15. R. R. HAKE, *Phys. Rev.* **158** (1967) 356.

Received 14 October
and accepted 15 December 1981